

Transition Metal Coordination Chemistry of N,N-Bis(2-(pyrid-2-ylethyl))hydroxylamine

Christopher W. Belock, Anil Çetin, Natalie V. Barone, and Christopher J. Ziegler*

Department of Chemistry, Knight Chemical Laboratory, University of Akron, Akron, Ohio 44325-3601

Received December 12, 2007

Although directly relevant to metal mediated biological nitrification as well as the coordination chemistry of peroxide, the metal complexes of hydroxylamines and their functionalized variants remain largely unexplored. The chelating hydroxylamine ligand N,N-bis(2-(pyrid-2-ylethyl))hydroxylamine can be readily generated via a solvent free reaction in high purity; however, the ligand is prone to decomposition which can hamper metal reaction. N,N-bis(2-(pyrid-2-ylethyl))hydroxylamine forms stable complexes with chromium(III), manganese(II), nickel(II), and cadmium(II) ions, coordinating in a side-on mode in the case of chromium and via the nitrogen in the case of the latter three metal ions. The hydroxylamine ligand can also be reduced to form N,N-bis(2-(pyrid-2-ylethyl))amine upon exposure to a stoichiometric amount of the metal salts cobalt(II) nitrate, vanadium(III) chloride, and iron(II) chloride. In the reaction with cobalt nitrate, the reduced ligand then chelates to the metal to form [N,N-bis(2-(pyrid-2-ylethyl))amine]dinitrocobalt(II). Upon reaction with vanadium(III) chloride and iron(III) chloride, the reduced ligand is isolated as the protonated free base, resulting from a metal-mediated decomposition reaction.

Introduction

The small molecule hydroxylamine (H_2NOH) can be considered either as a hybrid between water and ammonia or as a partially oxidized ammonia where a hydroxyl group is substituted for one of the hydrogen atoms.¹ Hydroxylamine is thus an intermediate between ammonia and nitrous oxide and nitrate and consequently is an important biological species. Hydroxylamine plays a role in biological nitrification, and it is oxidized to nitrite by the heme protein hydroxylamine oxidoreductase from the bacterium *Nitrosomonas europaea*.² This reaction can be reversed by siroheme-based nitrite reductases, where hydroxylamine once again is a stable intermediate.³ In electrochemistry, hydroxyl-

amine is a major product in the porphyrin mediated reduction of nitrate anion.⁴ Hydroxylamine is also used as a reductant in organic chemistry and alternatively can be reduced to form amines in reactions catalyzed by transition metals.^{1,5}

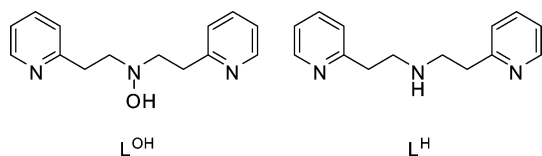
However, unlike NH_3 or NO , the coordination chemistry of hydroxylamine and its functionalized variants remains surprisingly unexplored. Several fundamental questions remain concerning the nature of hydroxylamine as a ligand, including the site of metal binding (N or O) and the protonation state of the OH group upon coordination. Unsubstituted hydroxylamine, however, often does not form stable metal complexes; while there are many examples of transition metal catalyzed hydroxylamine reactions, there are only 22 structures of unmodified hydroxylamine bound to a metal ion in the Cambridge Crystallographic Data Centre (CCDC) database, incorporating the elements V,⁶ Co,⁷ Mo,^{6e,8} Ru,⁹ W,¹⁰ Re,¹¹ Ir,¹² and U.¹³ One methodology to get around this problem is to functionalize either the oxygen or the nitrogen with R groups, which can result in the

* To whom correspondence should be addressed. E-mail: ziegler@uakron.edu.

- (1) (a) Benson, R. E.; Cairns, T. L.; Whitman, G. M. *J. Am. Chem. Soc.* **1956**, *78* (17), 4202–4205. (b) Jencks, W. P. *J. Am. Chem. Soc.* **1958**, *80* (17), 4581–4584. (c) Jencks, W. P. *J. Am. Chem. Soc.* **1958**, *80* (17), 4585–4588. (d) Jencks, P.; Gilchrist, M. *J. Am. Chem. Soc.* **1964**, *86* (24), 5616–5620.
- (2) (a) Rees, M. K. *Biochemistry* **1968**, *7* (1), 353–366. (b) Rees, M. K. *Biochemistry* **1968**, *7* (1), 366–372. (c) Hendrich, M. P.; Petasis, D.; Arciero, D. M.; Hooper, A. B. *J. Am. Chem. Soc.* **2001**, *123* (13), 2997–3005. (d) Kurnikov, I. V.; Ratner, M. A.; Pacheco, A. A. *Biochemistry* **2005**, *44* (6), 1856–1863.
- (3) Crane, B. R.; Siegel, L. M.; Getzoff, E. D. *Biochemistry* **1997**, *36* (40), 12101–12119.

- (4) (a) Barley, M. H.; Meyer, T. J. *J. Am. Chem. Soc.* **1986**, *108* (19), 5876–5885. (b) Younathan, J. N.; Wood, K. S.; Meyer, T. J. *Inorg. Chem.* **1992**, *31* (15), 3280–3285. (c) Choi, I.-K.; Liu, Y.; Wei, Z.; Ryan, M. D. *Inorg. Chem.* **1997**, *36* (14), 3113–3118.
- (5) Cicchi, S.; Bonanni, M.; Cardona, F.; Revuelta, J.; Goti, A. *Org. Lett.* **2003**, *5* (10), 1773–1776.

Scheme 1



formation of more stable complexes with metal ions. In addition, one can incorporate the hydroxylamine into a chelate to further stabilize metal coordination, as seen in the vanadium catalyst amavadine.¹⁴

In this report, we present the synthesis and characterization of a series of transition metal compounds with the ligand *N,N*-bis(2-(pyrid-2-ylethyl)hydroxylamine (L^{OH} , Scheme 1). We have examined the reaction chemistry of this species across the first row of the transition metals from vanadium to nickel, as well as the second row element cadmium. This work adds to the known complexes recently presented by Halcrow and co-workers.¹⁵ Previously, this ligand has exhibited two types of metal chemistries: complex formation via a *N,N'* tridentate binding mode or reduction to the *N,N*-bis(2-(pyrid-2-ylethyl)amine ligand (L^H). We have expanded this chemistry to several other transition metal ions to determine if these trends are observed across the periodic table and to probe whether a side-on binding mode is observed, as is seen in unmodified hydroxylamine. We have shown that this tridentate ligand can adopt different geometries upon metal binding and can bind through both the oxygen and the nitrogen atom. In addition, ligand reduction occurs more frequently than previously observed. The ligand

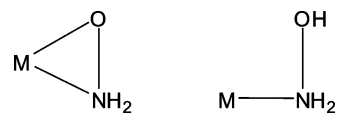


Figure 1. Observed modes of hydroxylamine metal binding.

is reduced in several of these reactions to form L^H , which can either chelate to a metal, as seen with cobalt, or can be isolated as the protonated free base.

Results and Discussion

On the basis of crystallographic evidence, unmodified hydroxylamine exhibits two types of metal binding. The ligand can bind either in a side-on fashion with deprotonation of the hydroxyl group or as N-bound with the hydroxyl group not participating in metal coordination (Figure 1). Of the previously elucidated complexes, only three compounds from the CCDC show N-bound hydroxylamine, as seen in [*trans*-Ru(CO)(NH₂OH)(PPh₃)₂(S₂CNEt₂)] [SO₃CF₃],⁹ [*mer,trans*-Re(CO)₃(NH₂OH)(PPh₃)₂] [SO₃CF₃],¹¹ and [Ir(μ -SC₆-H₃MeCH₂)Cl(PPh₃)(NH₂OH)]₂.¹² In these three structures, the N–O bond length measures 1.422(5), 1.45(1), and 1.432(5) Å, respectively. In gas phase hydroxylamine, the bond length is 1.453 Å, while in the inorganic salt [Ni(NH₂OH)₆] [SO₄] the average distance is 1.44 Å.¹⁶

In the side-on bound hydroxylamines, the N–O bond lengths are significantly shorter than those seen in the neutral form of ligand binding. The deprotonated form of hydroxylamine bears some structural similarities to peroxide⁶ and has been used to model the binding of this biologically relevant anion. A decade ago, Crans and co-workers presented a report on the vanadyl chemistry of hydroxylamine and isolated a number of vanadyl-hydroxylamine complexes.^{6c} All of the elucidated structures of hydroxylamine with the V=O unit are deprotonated and thus are hydroxylamido units. The mean N–O bond length for the known structures of bis-hydroxylamine vanadium complexes is approximately 1.40 Å, and the mono hydroxylamine has a slightly shorter N–O bond length (as seen in with the dipic ligand) of 1.371(4) Å. The V–O and V–N bonds are also similar in length, with mean values of approximately 1.90 and 2.02 Å, respectively. Crans proposed that the shortening of the N–O bond lengths results from ligand to metal charge transfer; however, an alternative interpretation would be that there is more double bond character in the N–O bond in free deprotonated hydroxylamine versus free protonated hydroxylamine (that is, there is some π bond character to the bond between the nitrogen and the oxygen). This unit can bind to the metal and engage in σ donation/ π acceptance similar to that seen in a side bound acyl group or carbonyl. In addition to the vanadium complexes, there also has been some limited structural work with the hydroxylamido ligand and the metals molybdenum, uranium, cobalt, and tungsten.^{7,8,10,13}

The ligand L^{OH} can be readily synthesized via the “solvent free” method described by Sayigh, Ulrich, and Green¹⁷

- (6) (a) Nuber, B.; Weiss, J. *Acta Crystallogr., Sect. B* **1981**, 37 (4), 947–948. (b) Paul, P. C.; Angus-Dunne, S. J.; Batchelor, R. J.; Einstein, F. W. B.; Tracey, A. S. *Can. J. Chem.* **1997**, 75 (2), 183–191. (c) Keramidias, A. D.; Miller, S. M.; Anderson, O. P.; Crans, D. C. *J. Am. Chem. Soc.* **1997**, 119 (38), 8901–8915. (d) Wiegardt, K.; Quilitzsch, U.; Nuber, B.; Weiss, J. *Angew. Chem., Int. Ed. Engl.* **1978**, 17 (5), 351–352. (e) Li, L.-Z.; Xu, T.; Wang, D.-Q. *J. Chem. Crystallogr.* **2004**, 34 (9), 585–590. (f) Hauser, C.; Weyhermuller, T.; Wiegardt, K. *Collect. Czech. Chem. Commun.* **2001**, 66 (1), 125–138.
- (7) Vogel, S.; Huttner, G.; Zsolnai, L.; Emmerich, C. *Z. Naturforsch., B: Chem. Sci.* **1993**, 48 (3), 353–363.
- (8) (a) Wiegardt, K.; Backes-Dehmann, G.; Swiridoff, W.; Weiss, J. *Inorg. Chem.* **1983**, 22 (8), 1221–1224. (b) Wiegardt, K.; Holzbach, W.; Weiss, J.; Nuber, B.; Prikner, B. *Angew. Chem., Int. Ed. Engl.* **1979**, 18 (7), 548–549. (c) Wiegardt, K.; Holzbach, W.; Nuber, B.; Weiss, J. *Chem. Ber.* **1980**, 113 (2), 629–638. (d) Sellmann, D.; Seubert, B.; Moll, M.; Knoch, F. *Angew. Chem., Int. Ed. Engl.* **1988**, 27 (9), 1164–1165. (e) Sellmann, D.; Seubert, B.; Knoch, F.; Moll, M. *Z. Naturforsch., B: Chem. Sci.* **1991**, 46 (11), 1449–1458.
- (9) Zheng, H.; Leung, W.-H.; Chim, J. L. C.; Lai, W.; Lam, C.-H.; Williams, I. D.; Wong, W.-T. *Inorg. Chim. Acta.* **2000**, 306 (2), 184–192.
- (10) Legzdins, P.; Rettig, S. J.; Sayers, S. F. *J. Am. Chem. Soc.* **1994**, 116 (26), 12105–12106.
- (11) Southern, J. S.; Hillhouse, G. L.; Rheingold, A. L. *J. Am. Chem. Soc.* **1997**, 119 (50), 12406–12407.
- (12) Matsukawa, S.; Kuwata, S.; Ishii, Y.; Hidai, M. *J. Chem. Soc., Dalton Trans.* **2002**, 13, 2737–2746.
- (13) (a) Schchelokov, R. N.; Orlova, I. M.; Beirakhov, A. G.; Mikhailov, Yu. N.; Kanishcheva, A. S. *Koord. Khim.* **1984**, 10 (12), 1644–1650. (b) Adrian, H. W. W.; Van Tets, A. *Acta Crystallogr., Sect. B: Struct. Crystallogr. Cryst. Chem.* **1978**, 34 (8), 2632–2634.
- (14) Reis, P. M.; Silva, J. A. L.; Palavra, A. F.; Fraústo da Silva, J. J. R.; Kitamura, T.; Fujiwara, Y.; Pombeiro, A. J. L. *Angew. Chem., Int. Ed.* **2003**, 42 (7), 821–823.
- (15) (a) Leaver, S. A.; Palaniandavar, M.; Kilner, C. A.; Halcrow, M. A. *J. Chem. Soc., Dalton Trans.* **2003**, No. 22, 4224–4225. (b) Leaver, S. A.; Kilner, C. A.; Halcrow, M. A. *Acta Crystallogr., Sect. C* **2004**, 60 (1), m1–m3.

- (16) Engelhardt, L. M.; Newman, P. W. G.; Raston, C. L.; White, A. H. *Aust. J. Chem.* **1974**, 27 (3), 503–507.

Table 1. Crystallographic Data Collection and Structure Parameters for Compounds **1–5**

	Cr(L ^O)Cl ₂ (1)	[MnCl(L ^{OH}) ₂ (μ-Cl) ₂] (2)	[Ni(L ^{OH})NO ₃ H ₂ O] (NO ₃) (3)	Cd(L ^{OH})(NO ₃) ₂ (4)	Co(L ^H)(NO ₃) ₂ (5)
formula	CrC ₁₄ H ₁₆ Cl ₂ N ₃ O	Mn ₂ C ₂₉ H ₃₄ Cl ₄ N ₆ O ₄	NiC ₁₄ H ₁₉ N ₅ O ₈	CdC ₁₄ H ₁₇ N ₅ O ₇	CoC ₁₄ H ₁₇ N ₅ O ₆
fw	365.20	782.30	444.05	479.73	409.25
cryst. syst.	monoclinic	triclinic	monoclinic	monoclinic	monoclinic
space group	<i>P</i> 2(1)/ <i>n</i>	<i>P</i> $\bar{1}$	<i>P</i> 2(1)	<i>P</i> 2(1)/ <i>c</i>	<i>P</i> 2(1)/ <i>c</i>
<i>a</i> (Å)	7.4880(10)	7.9509(19)	7.925(6)	8.1635(10)	8.4347(14)
<i>b</i> (Å)	13.2153(18)	9.206(2)	9.977(7)	26.122(3)	15.091(3)
<i>c</i> (Å)	15.329(2)	11.763(3)	12.264(9)	8.9873(11)	13.115(2)
α (deg)	90	82.708(4)	90	90	90
β (deg)	102.449(2)	77.339(4)	103.559(12)	115.271(2)	103.488(3)
γ (deg)	90	81.586(4)	90	90	90
vol, Å ³	1481.2(3)	827.0(3)	942.6(12)	1733.1(4)	1623.3(5)
<i>Z</i>	4	1	2	4	4
ρ (calc), Mg/m ³	1.638 Mg/m	1.571 Mg/m	1.564 Mg/m	1.839 Mg/m ³	1.675 Mg/m ³
μ , mm ⁻¹	1.134 mm ⁻¹	1.131 mm ⁻¹	1.082 mm ⁻¹	1.310	1.102
<i>F</i> (000)	748	400	460	960	840
reflns. collected	12699	7227	7946	15032	13824
indep. reflns.	3493	3742	4158	4080	3827
GOF on <i>F</i> ²	[<i>R</i> (int) = 0.0325]	[<i>R</i> (int) = 0.0265]	[<i>R</i> (int) = 0.0284]	[<i>R</i> (int) = 0.0400]	[<i>R</i> (int) = 0.0232]
<i>R</i> [<i>I</i> > 2 σ (<i>I</i>)]	1.047	1.054	0.998	1.086	1.084
<i>R</i> (all data)	R1 = 0.0299, wR2 = 0.0714	R1 = 0.0446, wR2 = 0.1126	R1 = 0.0344, wR2 = 0.0745	R1 = 0.0329, wR2 = 0.0752	R1 = 0.0316, wR2 = 0.0777
	R1 = 0.0353, wR2 = 0.0736	R1 = 0.0551, wR2 = 0.1186	R1 = 0.0385, wR2 = 0.0760	R1 = 0.0385, wR2 = 0.0774	R1 = 0.0355, wR2 = 0.0796

(although purification of the vinylpyridine requires solvent), which was based on the previous method developed by Bauer, Shoeb, and Agwada.¹⁸ This reaction produces a pure crystalline product, which is suitable for single crystal X-ray structure elucidation. The structure of the N,N-bis(2-{pyrid-2-ylethyl})hydroxylamine ligand has been recently elucidated by Bjernemose and Bond.¹⁹ We re-elucidated the structure as part of our characterization of this material, and our observations were identical to that of the previous structure. When working with this ligand, it is important to note that it is unstable and slowly decomposes over time at room temperature to an oily brown product, resulting from self-oxidation. The successful synthesis of metal complexes with L^{OH} was highly dependent on its purity. Thus, in all of our reactions we used freshly prepared ligand and always stored it in a freezer when not in use.

We examined reactions of L^{OH} with a variety of metals under mild conditions (room temperature, exposed to air) in methanol as the solvent. We examined this ligand with several first row transition metal salts (VCl₃, CrCl₃, MnCl₂, FeCl₃, Co(NO₃)₂, and Ni(NO₃)₂), as well as with the second row metal salt Cd(NO₃)₂. In all cases, the reactions produced crystalline products which could be characterized by single crystal X-ray diffraction. With four of the metal reagents studied, the ligand remained intact upon reaction, affording a complex of either neutral hydroxylamine or anionic hydroxylamide. However, the ligand was also just as likely to undergo decomposition upon reaction with a metal, typically to form the N,N-bis(2-{pyrid-2-ylethyl})amine (L^H). Both reaction types have been previously observed with this ligand by Halcrow and co-workers for the metals cobalt and copper, respectively.¹⁵ We shall first describe the reactions

where the ligand binds to the metal, as seen for chromium, manganese, nickel, and cadmium, followed by reactions where the ligand reductively decomposes upon exposure to a stoichiometric amount of metal salt. The data collection and structure parameters for the products (compounds **1–5**) from the reactions with CrCl₃, MnCl₂, Ni(NO₃)₂, Cd(NO₃)₂, and Co(NO₃)₂ are listed in Table 1, and the data from crystals from the reactions with VCl₃ and FeCl₃ are presented as Supporting Information. In short, with these metal ions, we observe four types of chemistries: tridentate coordination of L^{OH} to the metal with retention of the proton on the hydroxylamine oxygen, tetradentate coordination of L^{OH} to a metal in a side-on deprotonated mode, reduction of the hydroxylamine and tridentate coordination, and reduction of the amine without metal coordination.

With the metals chromium, manganese, nickel and cadmium, the ligand remained intact upon reaction with the metal salt, and the structures of these complexes are shown in Figure 2. The chromium adduct (**1**) has the formula Cr(L^O)Cl₂ and is formed from the reaction of CrCl₃ and the free base ligand in methanol solution. The metal remains in the +3 oxidation state, with charge balance being provided by two chlorides and the deprotonation of the hydroxyl group of the ligand. The metal is six coordinate, with the two pyridyl groups binding along the axial ordinate and the N–O unit bound side-on in an equatorial position. The remaining two equatorial positions are occupied by chlorides. As a result, the geometry is a distorted octahedron because of the small bite angle of the side-on bound N–O unit. In the N–O chelate, the Cr–O distance (1.9193(13) Å) is appreciably closer than the Cr–N distance (1.9686(15) Å). This binding mode is similar to that seen in the vanadyl complexes of hydroxylamine.⁶ As in the vanadyl analogs, the binding of the N–O unit results in a shortening of the N–O bond from 1.4504(16) Å in the free base species to a distance of 1.4031(18) Å in the chromium complex.

(17) Sayigh, A. A. R.; Ulrich, H.; Green, M. *J. Org. Chem.* **1964**, *29* (7), 2042–2043.

(18) Bauer, L.; Shoeb, A.; Agwada, V. C. *J. Org. Chem.* **1962**, *27* (9), 3153–3155.

(19) Bjernemose, J. K.; Bond, A. D. *Acta Crystallogr. Sect. E* **2004**, *60* (7), o1143–o1144.

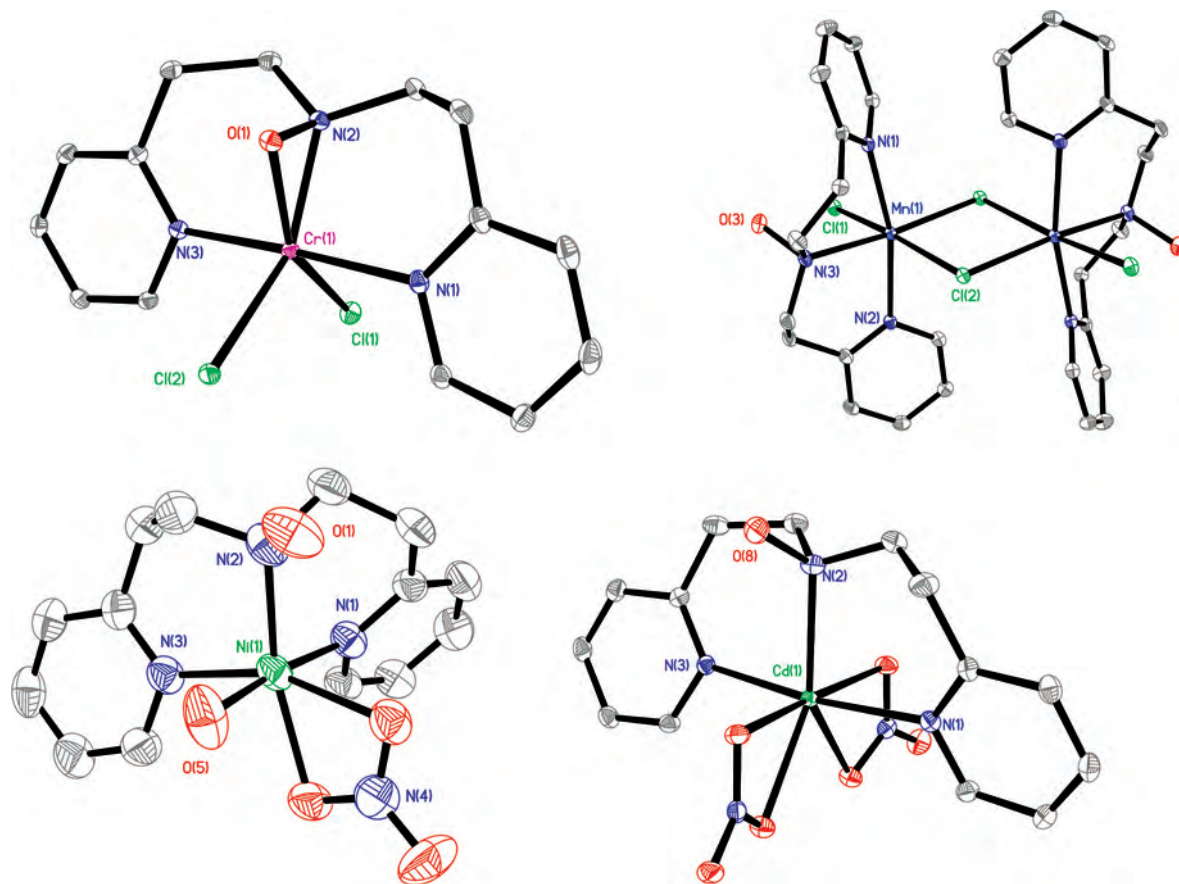


Figure 2. Structures of $\text{Cr}(\text{L}^{\text{O}})\text{Cl}_2$ (**1**, top left), $[\text{MnCl}(\text{L}^{\text{OH}})]_2(\mu\text{-Cl})_2$ (**2**, top right), the cation of $[\text{Ni}(\text{L}^{\text{OH}})(\text{H}_2\text{O})(\text{NO}_3)](\text{NO}_3)$ (**3**, bottom left), and $\text{Cd}(\text{L}^{\text{OH}})(\text{NO}_3)_2$ (**4**, bottom right). Hydrogen atoms have been omitted for clarity. The thermal ellipsoids for compounds **1**, **2**, and **4** are rendered at the 35% level, while the ellipsoids for **3** are rendered at the 50% level.

The magnetic susceptibility measurements indicate that the metal is a Cr(III) complex, with three unpaired electrons ($\mu_{\text{eff}} = 3.8$). The UV–visible spectrum in methanol shows two peaks at 539 and 371 nm, with extinction coefficients of 57.4 and 50.5 $\text{M}^{-1} \text{cm}^{-1}$, respectively. Because the complex has a distorted octahedral coordination environment for a d^3 metal ion, the lowest energy transition (18550 cm^{-1}) is approximately equal to the Δ_{O} . This value is intermediate between aqua $\text{Cr}(\text{H}_2\text{O})_6^{3+}$ ($17\,400 \text{ cm}^{-1}$) and $\text{Cr}(\text{NH}_3)_6^{3+}$ ($21\,250 \text{ cm}^{-1}$) and indicates a ligand field of moderate strength on the spectrochemical series. The Electron Paramagnetic Resonance (EPR) spectrum of $\text{Cr}(\text{L}^{\text{O}})\text{Cl}_2$ is shown in Figure 3, and it confirms the spin state assignment from the magnetic susceptibility measurements. The spectrum exhibits features that correspond to a complex with intermediate to large zero field splitting of the $S = 3/2$ ground state, based on typical patterns seen in Cr(III) systems.²⁰

The product of the ligand reaction with manganese(II) chloride results in a dimeric Mn(II) complex (**2**) of the formula $[\text{MnCl}(\text{L}^{\text{OH}})]_2(\mu\text{-Cl})_2$. The elucidated structure has a single solvent methanol per formula unit in the unit cell, with the oxygen atom occupying a special position. Two manganese(II) metal ions and two chlorides form a diamond core structure, with a Cl–Mn–Cl angle of $82.84(3)^\circ$ and a Mn–Cl–Mn angle of $97.16(3)^\circ$. The dimer is symmetric

around the core, and the coordination environment about each metal also contains a terminal chloride, resulting in an octahedral coordination environment with the ligand in a meridional configuration. Unlike the chromium complex, the N–O unit binds through the nitrogen atom, and the oxygen remains protonated upon metal binding. The Mn–N bond distances in **2** are relatively long, with values of $2.271(2) \text{ \AA}$ and $2.281(2) \text{ \AA}$ for the pyridines and $2.343(2) \text{ \AA}$ for the hydroxylamine nitrogen. The binding of the hydroxylamine through the nitrogen does lengthen the N–O bond versus that of the free ligand to $1.469(3) \text{ \AA}$.

Magnetic susceptibility measurements indicate that **2** is paramagnetic, ($\mu_{\text{eff}} = 8.2$ for the dimer). There have been several studies of Mn(II)₂Cl₂ dimeric complexes that incorporate tridentate ligands, and these compounds can exhibit either ferromagnetic or antiferromagnetic interactions between the metal centers.²¹ Our observed susceptibility is very similar to that seen by Reedijk in the structurally analogous N-(3-methoxypropyl)-N,N-bis(pyridine-2-ylmethyl)-amine (mpbpa) complex $[\text{MnCl}(\mu\text{-Cl})(\text{mpbpa})]_2$, which has a $\mu_{\text{eff}} = 8.58$ at 300 K.²² This complex, composed of two high spin Mn(II) ions, exhibits ferromagnetism and has an observed J of 0.55 cm^{-1} . We are continuing our investigation

(21) Qi, C.-M.; Sun, X.-X.; Gao, S.; Ma, S.-L.; Yuan, D.-Q.; Fan, C.-H.; Huang, H.-B.; Zhu, W.-X. *Eur. J. Inorg. Chem.* **2007**, 3663–3668.

(22) Wu, J.-Z.; Bouwman, E.; Mills, A. M.; Spek, A. L.; Reedijk, J. *Inorg. Chim. Acta* **2004**, 357, 2694–2702.

(20) Petersen, E.; Toftlund, H. *Inorg. Chem.* **1974**, 13 (7), 1603–1612.

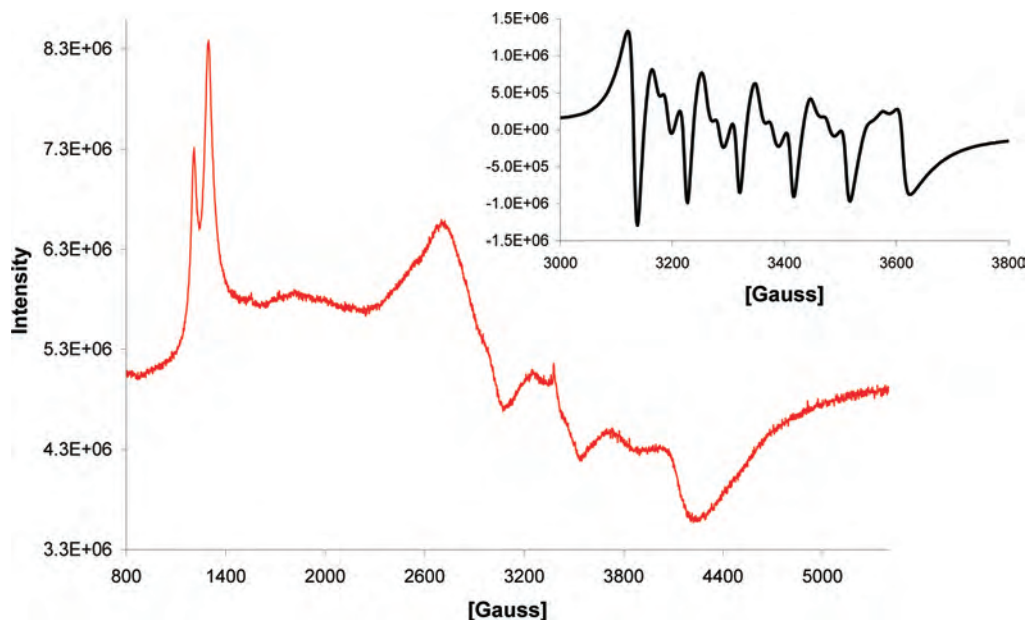


Figure 3. EPR spectra of $\text{Cr}(\text{L}^{\text{OH}})\text{Cl}_2$ (**1**) and $[\text{MnCl}(\text{L}^{\text{OH}})_2(\mu\text{-Cl})_2]$ (**2**, inset) in frozen MeOH/toluene at 120K.

into the magnetic properties of this complex and are in the process of obtaining variable temperature and field susceptibility data.

The absorption spectrum of this complex in methanol is in agreement with a high spin assignment, since there are no bands present in the 350–800 nm range. In addition, there are long metal–ligand bond distances in this complex, which indicate that the metal center has a high spin ground state. EPR spectra of the dimer complex in methanol/toluene at 298–115 K (Figure 3) show a six line splitting pattern. This pattern results from splitting with the $I = 5/2$ of the $^{55}\text{Mn}(\text{II})$ nucleus and is similar to that seen for other $\text{Mn}(\text{II})_2\text{Cl}_2$ dinuclear complexes. At room temperature, only the six line splitting is observed but as the temperature is lowered increased fine structure can be observed in the splitting pattern.

The reaction of L^{OH} with $\text{Ni}(\text{NO}_3)_2$ produces navy blue crystals of compound **3** $[\text{Ni}(\text{L}^{\text{OH}})(\text{H}_2\text{O})(\text{NO}_3)](\text{NO}_3)$, in good yield (66%). The structure of this complex was elucidated by single crystal X-ray methods; however, the crystal undergoes a phase transition below 150 K. As a result only high temperature data was obtained for this material. The compound is a cationic, six-coordinate, monometallic complex with the three nitrogens of the ligand binding to the metal in a facial configuration, in contrast to the meridonal geometries seen in chromium, manganese, and cadmium (vide infra) complexes. The Ni–N bonds are 2.063(3) and 2.049(3) Å for the pyridyl nitrogens and 2.064(2) Å for the hydroxylamine nitrogen. The N–O bond is 1.457(3) Å, which is closer to the bond length in free ligand. The remainder of the coordination sphere is occupied by a nearly symmetric bidentate nitrate and a solvent water, creating a geometry that is intermediate between octahedral and trigonal bipyramidal (if one were to treat the bidentate nitrate as a monodentate ligand). It is interesting to note that the complex is chiral and crystallizes out in the $P2(1)$ space group, with crystals of each enantiomer. A second equivalent of nitrate

is found in the asymmetric unit, providing charge balance for the cationic complex. The hydroxide of the NOH unit is not bound to the metal and remains protonated, as seen in the manganese dimer species. Previously, Halcrow and co-workers reported the complex of L^{OH} with NiCl_2 and, on the basis of spectroscopic data, proposed a structure similar to that of the complex of L^{OH} with CoCl_2 , where the ligand adopts a meridonal type geometry.¹⁵

Complex **3** is paramagnetic and exhibits a magnetic susceptibility of $\mu_{\text{eff}} = 2.5$, which is indicative of a $S = 1$ metal complex. The UV–visible spectrum shows two peaks at 591 and 368 nm, with extinction coefficients of 24.0 and $50.7 \text{ M}^{-1} \text{ cm}^{-1}$, respectively. As in the chromium compound, the lowest energy transition is approximately equivalent to the Δ_{O} for a distorted octahedral environment, and the energy of this band is equal to $16\,920 \text{ cm}^{-1}$. The nickel complex does not show a readily observable EPR spectrum at room temperature or at 120 K, which is not surprising since this is not a Kramer's doublet system.

We also investigated the chelation of the L^{OH} ligand to the second row element cadmium. The reaction of this ligand with $\text{Cd}(\text{NO}_3)_2$ affords yellow crystals of $\text{Cd}(\text{L}^{\text{OH}})(\text{NO}_3)_2$ (**4**) in ~50% yield. The structure of the compound shows a neutral complex, with a tridentate ligand binding to the metal through the nitrogen atoms in a meridonal geometry. The coordination number for this complex is seven, with the remaining coordination sphere occupied by two asymmetric bidentate nitrates. The Cd–N bonds are 2.317(2) and 2.332(2) Å for the pyridyl nitrogens and 2.325(3) Å for the hydroxylamine nitrogen. The hydroxylamine N–O bond is longer than that seen for the free ligand, with a length of 1.462(3) Å. This complex is diamagnetic and affords a readily interpretable ^1H NMR spectrum that is virtually identical to that of the free hydroxylamine and reflects the symmetric nature of the ligand binding.

In addition to affording metal complexes with the unmodified ligand, the L^{OH} ligand also frequently is reduced by

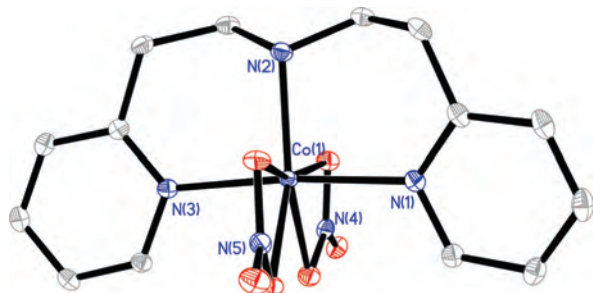


Figure 4. Structure of $\text{Co}(\text{L}^{\text{H}})(\text{NO}_3)_2$ (**5**) rendered with 35% thermal ellipsoids. Hydrogen atoms have been omitted for clarity.

transition metal ions to produce N,N-bis(2-(pyrid-2-ylethyl)amine. This reaction was first noticed by Halcrow and co-workers,¹⁵ and at that time the authors noted that this reduction could be utilized for facile production of the amine. We have confirmed this observation with three different metal salts: VCl_3 , FeCl_3 , and $\text{Co}(\text{NO}_3)_2$. In the case of the first two reagents, work up of the reaction produces a mixture of products, including crystals of the protonated ligand, which were elucidated by single crystal X-ray methods. For the VCl_3 reaction, the counterion is chloride, while for the FeCl_3 reaction, the counterion is the FeCl_4^- monoanion. In both cases, it appears that the metal is mediating the ligand self-oxidation reaction and is not oxidized by the hydroxylamine. While we cannot entirely rule out metal oxidation based on the evidence presented in this report, the self-oxidation conclusion is based on the observed lack of stability of the L^{OH} ligand, the lack of oxidation of the metal in the FeCl_3 reaction, and the >50% yields obtained in these reactions. Studies of the decomposition of the L^{OH} ligand are ongoing with redox inactive ligands, such as Zn^{2+} .

In the case of $\text{Co}(\text{NO}_3)_2$, the ligand is reduced and chelates to the metal, forming the compound $\text{Co}(\text{L}^{\text{H}})(\text{NO}_3)_2$ (**5**). The structure of this complex is shown in Figure 4. Based on yield alone, this reaction is apparently not stoichiometric, and the product yield is 38%. The complex is globally similar to the complex of L^{OH} with Co(II) previously described by Halcrow.¹⁵ The primary differences between the two structures are the reduction of the ligand, the substitution of two symmetric bidentate nitrates for chlorides, and the subsequent increase in coordination number at the metal to seven. In addition, the Co–N bonds of the bound pyridyl groups are slightly shorter than those seen in $\text{Co}(\text{L}^{\text{OH}})\text{Cl}_2$: 2.1324(15) and 2.1376(15) Å versus 2.1751(13) and 2.1731(12) Å.¹⁵ Interestingly, the Co–N bond to the amine unit is essentially identical to that of the dichloride, with a distance of 2.0984(15). The geometry of **5** is also very similar to that seen in the above-described cadmium complex; the nitrates bind in an asymmetric bidentate fashion, completing the coordination sphere around the metal.

Magnetic susceptibility studies of this complex confirm that the cobalt is in the +2 oxidation state, with a $\mu_{\text{eff}} = 4.2$ that is indicative of a $S = 3/2$ ion. The ^1H NMR of the complex shows resonances that are clearly broadened and shifted by the paramagnetic metal center. The EPR spectrum of **5** at 120 K shows only a weak signal because of spin

relaxation problems associated with the 3/2 ground state. The UV–visible spectrum displays a peak at 508 nm with two shoulders; the spectrum is in agreement with previously characterized $\text{Co}(\text{L}^{\text{H}})\text{X}_2$ complexes reported by Madden and Nelson.²³

Halcrow does present a structure where the ligand is reduced to form the amine; this is observed upon reaction of L^{OH} with Cu(II) salts. Initially, with chloride as the counterion, the complex of the hydroxylamine can be isolated, but eventually the ligand is reduced to form the N,N-bis(2-(pyrid-2-ylethyl)amine complex of Cu(II). Halcrow reported that this reaction appeared to be copper specific and that it did not occur with the other metals investigated in his report (specifically Ni and Co). In this work, we have observed that the reduction of hydroxylamine by metal is common and can occur with multiple first row metals.

In conclusion, stable hydroxylamine complexes of transition metals can be readily synthesized through simple chelation reactions. The ligand can bind to metals in both facial and meridional geometries, and the hydroxylamine can bind through the amine as the neutral form or side-on when deprotonated. In addition, the ligand is also very susceptible to decomposition under the conditions used in these syntheses. Typically, reduction of the ligand can take place to form the bis(2-ethylpyridyl)amine, which can crystallize as a protonated salt or can chelate to a metal as observed with Co(II). Based on this work and that of Halcrow and co-workers,¹⁵ the use of metal salts to reduce hydroxylamine may be a facile method for generating N,N-bis(2-(pyrid-2-ylethyl)amine.

Experimental Section

General Experimental Methods. All chemicals were purchased from Sigma-Aldrich or Lancaster and used as received. All ^1H and ^{13}C NMR spectra were recorded on Varian VXR or GEMINI spectrometers at 300 and 75 MHz in CDCl_3 , respectively. The CDCl_3 peak was used as an internal standard (7.27 ppm for ^1H and 77.23 ppm for ^{13}C). Absorption experiments were carried out on a Hitachi 3310 single monochromator spectrophotometer, and either methanol or chloroform was chosen as the solvent. High resolution mass spectrometry experiments were performed at the Mass Spectrometry and Proteomics Facility of Ohio State University on a Micromass ESI-ToF II (Micromass, Wythenshawe, U.K.) mass spectrometer equipped with an orthogonal electrospray source (Z-spray) operated in positive ion mode. Sodium iodide was used for mass calibration for a calibration range of m/z 100–2000. Samples were prepared in a solution containing acidified methanol and infused into the electrospray source at a rate of 5–10 $\mu\text{L min}^{-1}$. Optimal ESI conditions were as follows: capillary voltage 3000 V, source temperature 110 °C, and a cone voltage of 55 V. The ESI gas was nitrogen. Data were acquired in continuum mode until acceptable averaged data were obtained. X-ray intensity data were measured at 100 K (Bruker KYRO-FLEX) on a Bruker SMART APEX CCD-based X-ray diffractometer system equipped with a Mo-target X-ray tube ($\lambda = 0.71073$ Å) operated at 2000 W power. The crystal was mounted on a cryoloop using Paratone N-Exxon oil and placed under a steam of nitrogen at 100 K. The detector was placed at a distance of 5.009 cm from the crystal. Elemental

(23) Madden, D. P.; Nelson, S. M. *J. Chem. Soc. A* **1968**, 2342–2348.

analysis was conducted at the University of Illinois, School of Chemical Sciences Microanalysis Laboratory. Crystals were air-dried prior to elemental analysis. EPR spectra were collected on a Bruker ELEXSYS E-500 system.

Synthesis of N,N-Bis(2-{pyrid-2-ylethyl})hydroxylamine (L^{OH}). This procedure was based on the reaction described by Agwada et al. A mixture of 2-vinylpyridine (16.2 mL, 1.50×10^{-1} mol) was purified by dissolution in CH₂Cl₂ and filtration through a silica plug, followed by removal of the solvent. Hydroxylamine hydrochloride (8.35 g, 1.20×10^{-1} mol) was added to the purified 2-vinylpyridine and allowed to stand overnight. The solution was neutralized with NaHCO₃ followed by an extraction with CHCl₃; the solution was dried using MgSO₄ and excess 2-vinylpyridine removed by rotary evaporation. The resultant product was recrystallized from CH₂Cl₂ and hexane. Characterization, including ¹H NMR, high res. ESI MS, and single crystal X-ray analysis, were identical to previously published data. Yield 4.07 g, 24.4%.

Synthesis of DichloroN,N-bis(2-{pyrid-2-ylethyl})hydroxylaminechromium(II) Cr(L^{OH})(Cl₂), 1. A solution of L^{OH} (0.0475 g, 1.88×10^{-4} mol) in 3.5 mL of MeOH was mixed with a solution of Cr(Cl₃)·6H₂O (0.050 g, 1.9×10^{-4} mol) in 3.5 mL MeOH and was stirred at room temperature for 5 min. The solution immediately turned to a blue color. This solution was diffused with a Et₂O vapor overnight, resulting in the formation of a grayish blue crystals suitable for X-ray diffraction. Yield 1.0×10^{-2} g, (22%). High res. ESI MS (positive ion): 329.0 *m/z* (M – Cl[–]) CHN Anal. Calcd for CrN₃OCl₄H₁₆Cl₂: C, 46.04; H, 4.42; N, 11.51. Found: C, 46.10; H, 4.38; N, 11.24. IR (cm^{–1}): 1609, 1568, 1440, 1028, 893, 777, 758, 735, 687, 678. X-ray crystallography: Crystal data and structure refinement parameters are summarized in Table 1.

Synthesis of μ-Dichlorobis[N,N-bis(2-{pyrid-2-ylethyl})hydroxylaminemanganese(II)] [Mn(L^{OH})Cl₂](Cl₂), 2. The same method was used as in 1, with Mn(Cl₂)·4H₂O (0.050 g, 2.5×10^{-4} mol) and L^{OH} (0.064 g, 2.526×10^{-4} mol). Yellow crystals suitable for single crystal X-ray diffraction formed from the Et₂O diffusion solution. Yield 9.8×10^{-3} g, (20%). High res. ESI MS (positive ion): 703.054 *m/z* (M – Cl[–]). CHN Anal. Calcd for Mn₂N₆O₂C₂₈H₃₄Cl₂: C, 45.55; H, 4.64; N, 11.38. Found: C, 45.11; H, 5.03; N, 10.70. IR (cm^{–1}): 3236, 1604, 1568, 1485, 1444, 1393, 1321, 1156, 1108, 1064, 1027, 1016, 865, 782, 712, 686, 678. X-ray crystallography: Crystal data and structure refinement parameters are summarized in Table 1.

Synthesis of [AquaN,N-bis(2-{pyrid-2-ylethyl})nitronickel(II)]-nitrate ([Ni(L^{OH})(NO₃)H₂O)](NO₃), 3. The same method was used as in 1, with Ni(NO₃)₂·6H₂O (0.036 g, 9.2×10^{-5} mol) and L^{OH} (0.050 g, 1.9×10^{-4} mol). Blue single crystals suitable for X-ray diffraction formed upon diffusion with Et₂O. Yield 0.029, (66%).

High res. ESI MS (positive ion): 466.1 *m/z* (M + Na⁺). CHN Anal. Calcd for NiN₅O₇C₁₄H₁₉: C, 37.87; H, 4.31; N, 15.77. Found: C, 38.31; H, 4.26; N, 15.36. IR (cm^{–1}): 3452, 3145, 1609, 1571, 1482, 1447, 1409, 1305, 1158, 1108, 1070, 1026, 902, 826, 809, 787, 771, 678. X-ray crystallography: Crystal data and structure refinement parameters are summarized in Table 1.

Synthesis of N,N-Bis(2-{pyrid-2-ylethyl})hydroxylamine-dinitrocadmium(II) (Cd(L^{OH})(NO₃)₂), 4. The same method was used as in 1, with Cd(NO₃)₂·6H₂O (0.050 g, 1.453×10^{-4} mol) and L^{OH} (0.0368 g, 1.453×10^{-4} mol). Yellow crystals suitable for X-ray diffraction formed upon diffusion with Et₂O. Yield 0.018 g, (50%). ¹H NMR (DMSO, δ): 2.95 (s, 2H, -CH₂), 7.20 (t, 1H, ArH), 7.26 (d, 1H, ArH), 7.98 (s, 1H, -OH), 8.45 (d, 1H, ArH). High res. ESI MS (positive ion): 419.0 (M – NO₃[–]). CHN Anal. Calcd for CdN₅O₇C₁₄H₁₇: C, 35.05; H, 3.57; N, 14.60. Found: C, 35.13; H, 3.58; N, 14.16. IR (cm^{–1}): 3334, 1606, 1570, 1464, 1442, 1407, 1386, 1313, 1284, 1164, 1109, 1049, 1034, 1015, 987, 884, 794, 766. X-ray crystallography: Crystal data and structure refinement parameters are summarized in Table 1.

Synthesis of [N,N-Bis(2-{pyrid-2-ylethyl})amine]dinitrocobalt(II) Co(L^H)(NO₃)₂, 5. The same method was used as in 1, with Co(NO₃)₂·6H₂O (0.050 g, 1.7×10^{-4} mol) and L^{OH} (0.044 g, 1.7×10^{-4} mol). Red-purple crystals suitable for X-ray diffraction formed upon diffusion with Et₂O. Yield 0.013 (31%). High res. ESI MS (positive ion): 428.9 (M + H₃O⁺). Anal. Calcd for CoN₅O₆C₁₄H₁₇: C, 41.99; H, 4.18; N, 17.07. Found: C, 41.36; H, 4.22; N, 16.84. IR (cm^{–1}): 3249, 2875, 1608, 1571, 1477, 1444, 1317, 1298, 1178, 1162, 1114, 1091, 1030, 981, 835, 814, 778, 766, 735, 686. X-ray crystallography: Crystal data and structure refinement parameters are summarized in Table 1.

Acknowledgment. The authors wish acknowledge NSF Grant CHE-0116041 for funds used to purchase the Bruker-Nonius diffractometer, NSF Grant CHE-0420987 for funds used to purchase the Bruker EPR spectrometer and the Kresge Foundation and donors to the Kresge Challenge Program at The University of Akron for funds used to purchase the NMR instrument used in this work.

Supporting Information Available: Experimental details on the reactions of L^{OH} with FeCl₃ and VCl₃, crystal structures of L^{OH} and protonated L^H from the FeCl₃ and VCl₃ reactions, and UV–visible spectra of compounds 1, 3, and 5. This material is available free of charge via the Internet at <http://pubs.acs.org>.

IC702406N